Rapidly Developing Cumulus Areas Derivation Algorithm Theoretical Basis Document

RDCA

March 2012

Meteorological Satellite Center/JMA

・Version Info.

Ver. 0.99　March 2012　A. Sobajima

1. Introduction of New Product "Rapidly Developing Cumulus Area (RDCA)"

1-1. Back Ground and Objective

"Rapidly Developing Cumulus Area (RDCA)" is one of the nowcast products for aviation users. Objective of this product is safety for aviation operation as a result of detecting rapidly developing convective clouds earlier than Radar or other observations detect nimbus. MTSAT-1R images at the interval of 5 minutes are used to produce RDCA.

Geostationary meteorological satellites have contributed to observation of meteorological phenomena from synoptic scale to mesoscale because of their large coverage. And they are used to calculate data as typified by Atmospheric Motion Vectors, which are crucial for numerical weather prediction, and to provide a wide variety of products such as sea surface temperature and monitoring yellow sand that are important to monitor the earth's environment. Recent years, hardware of satellite is improved and short time interval observation (rapid scan observation) becomes available by observing comparatively narrow area in repetitive manner. MTSAT-1R, which is in Himawari series and started operating in 2005, has function of rapid scan observation. Geostationary meteorological satellite JMA operates have been called Himawari in Japan. In 2011, MTSAT-1R started rapid scan observation while standby operation.

Short time weather forecast (nowcast) using rapid scan observation of geostationary meteorological satellite has began in many parts of the world. Representative product is CI (Convective Initiation) by EUMETSAT. The CI makes use of detection parameters based on time variation ratio of VIS, IR, difference of IR and cloud particle radius distribution inference near cloud top that are obtained by 12 channel data of Meteosat (EUMETSAT 2007; Mecikalski and Bedka 2006). Also NOAA carries forward development and utilization of products. It is aimed to detect cumulus and cumulus nimbus clouds which bring severe phenomenon by upgrading geostationary meteorological satellite observation.

In this document, algorithm, score and future problems of RDCA as of March 2012 are described. However, detection of cumulus nimbus cloud area which is a part of Cumulus Nimbus Area Information Product is not described in this document.

1-2. Overview of Rapid Scan Observation and Service Schedule of RDCA

Fig. 1.1 shows timetable of rapid scan observation by MTSAT-1R from 2011. Observation is operated 5 minutes interval basically, but north hemisphere observation

is carried out every 2 hours in order to get navigation accuracy. Fig. 1.2 shows rapid scan observational range. This range is fixed. Along this schedule RDCA is got executed and product is distributed from 00:10 UTC to 08:55 UTC. However, RDCA detection process will be terminated by algorithmic restriction solar zenith angle is greater than 75 degrees (later discussion).

Table1.1 shows central wavelength of all channels of MTSAT-1R. This abbreviation is used in explanation of RADA algorithm in what follows.

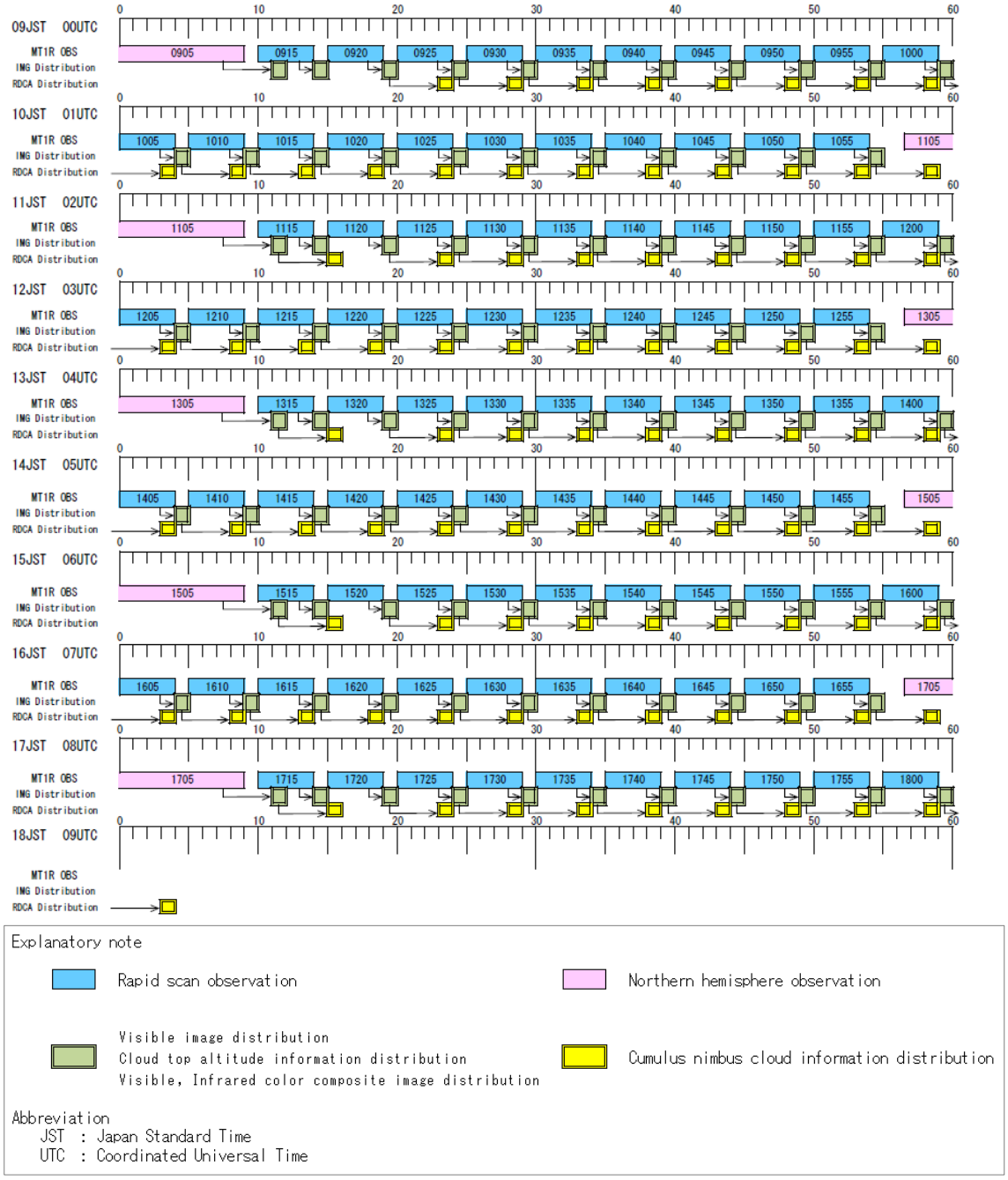

Fig. 1.1 Timetable of rapid scan observation.

Observation is carried out at 5 minutes interval by MTSAT-1R.

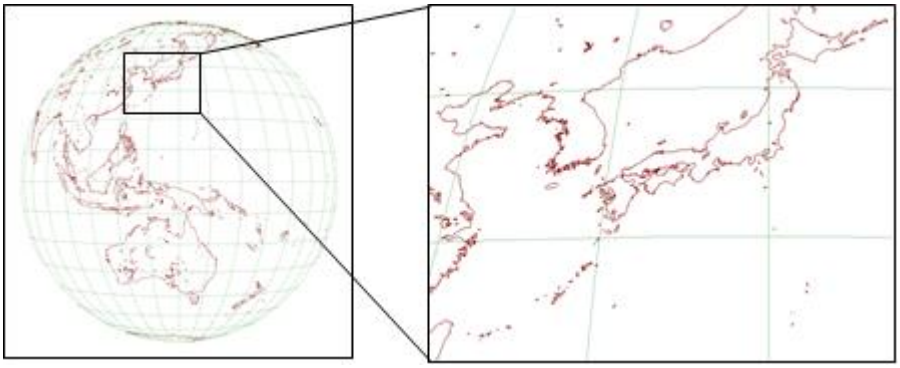

Fig. 1.2 Observation range of rapid scan (5 minutes interval) by MTSAT-1R.

Table 1.1 Central wavelength and abbreviation of MTSAT-1R.

Channel	Central Wavelength(μm)
VIS	0.65
IR1	10.8
IR2	12.0
IR3	6.8
IR4	3.8

1-3. Outline of processing flow about RDCA

Fig. 1.3 shows processing flow of RDCA. The process consists of three steps. By the way, there is drawing process at final step after the third step. Explanation of drawing process is omitted from this document because it is integrative process including cumulus nimbus cloud detection process.

1. Extract Detection Area (Preprocessing).
2. Calculate Detection Parameter.
3. Calculate Prediction Index.

Pixels as object of detection are extracted from whole image in process No. 1. Cloud characteristics of its development level, which comes out of MTSAT-1R VIS or IR imagery, are quantified as parameters for these extracted pixels in No. 2 process. In process No. 3, these parameters are indexed by logistic regression analysis. Pixels are determined if rapidly developing cloud is detected or not by using this index. In the next section, these detection methods are detailed.

1-4. Outline of Cumulus Nimbus Cloud Information

Result of RDCA is provided to aviation user as a part of Cumulus Nimbus Cloud Information noted above. Outline of Cumulus Nimbus Cloud Information is discussed in this section.

Results of Rapidly Developing Cloud Area and Cumulus Nimbus Cloud Detection is displayed simultaneously on background of VIS imagery (or IR1 imagery in case of sun zenith angle is over 75 degrees) in Cumulus Nimbus Cloud Information. Rapidly Developing Cloud Area is colored with green, Cumulus Nimbus Cloud Detection is colored with red, and unclear area of lower or middle cloud is colored with aqua. Unclear area stands for lower level cloud or middle level cloud are not able to be acquired because of dense anvil cloud at the stage of peak or decay cumulus nimbus cloud.

Detection process of RDCA makes use of parameters from VIS imagery, detection accuracy turns down consequently when sun zenith angle grows up. Therefore detection of RDCA is not carried out where sun zenith angle is over 75 degrees.

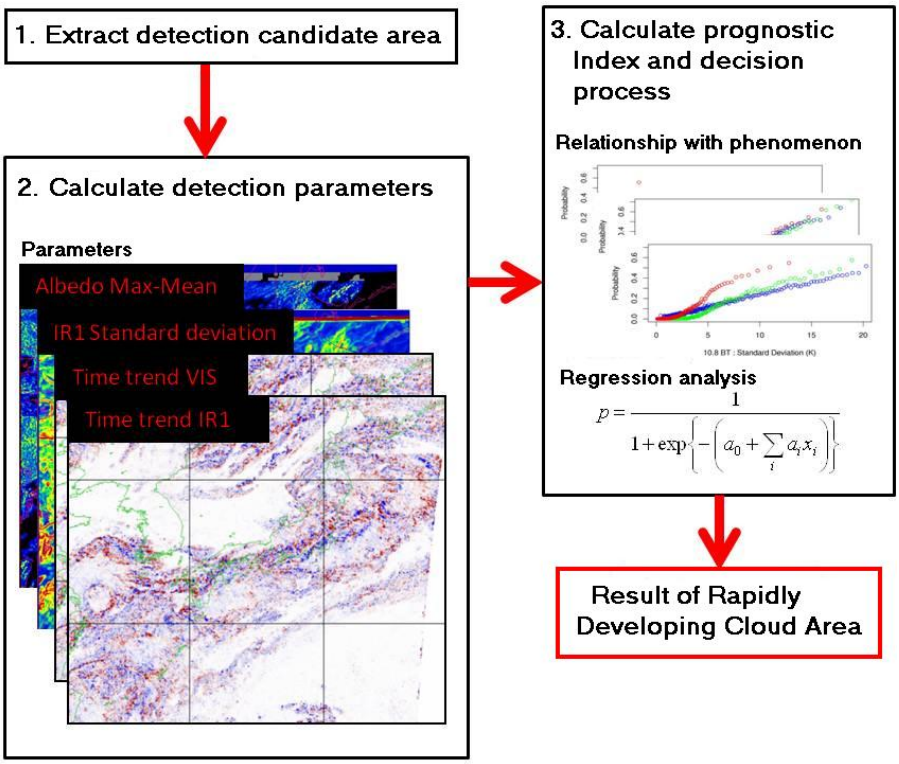

Fig. 1.3 Processing flow of RDCA (Conceptual Diagram).

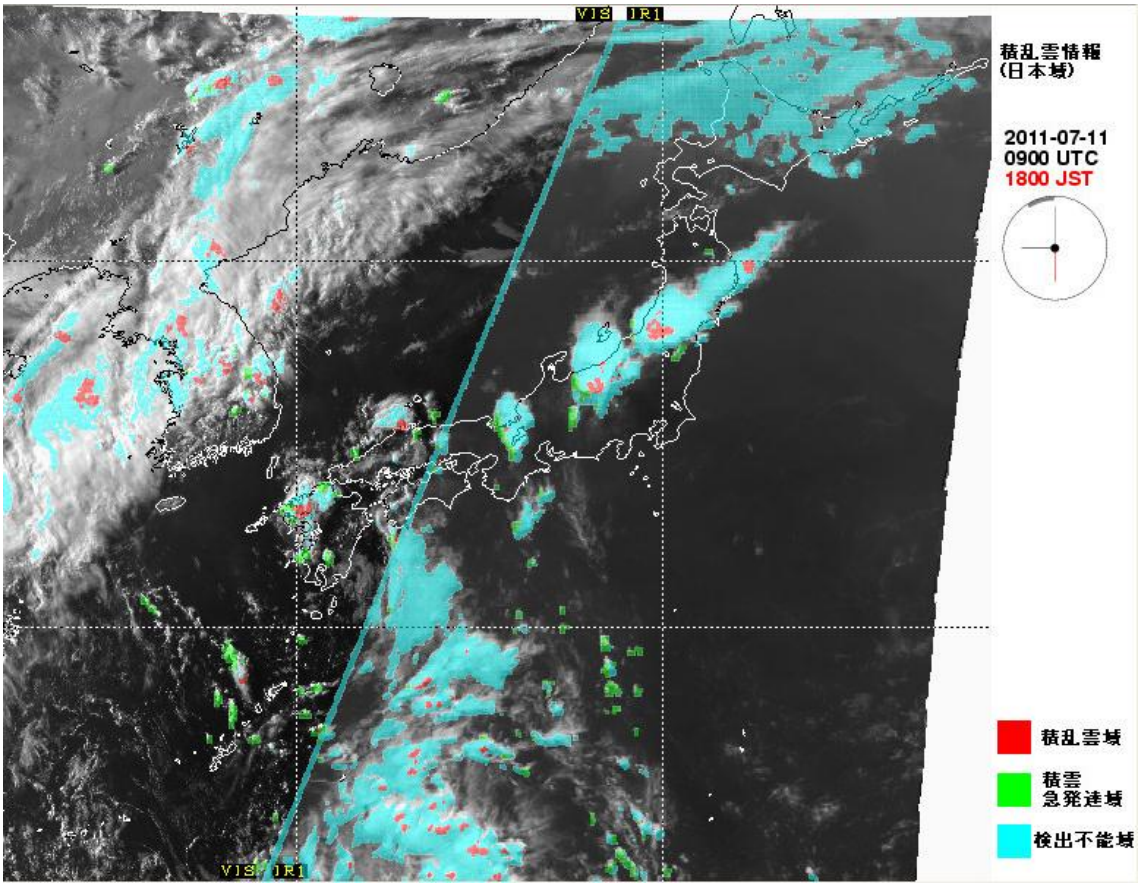

Fig. 1.4 Sample of cumulus nimbus information.

Rapidly developing cloud area is colored with green.

Line of image center is corresponding to solar zenith angle75 degrees.

2. Algorithm of Rapidly Developing Cloud Area Detection

All channels shown in Table 1.1 are used in detection processes. On this occasion, detection processes make use of projection transformed squared grid IR/VIS imagery from 121 to 149 degrees east longitude, from 23 to 47 degrees north latitude.

2-1. Extracting detection candidate area (preprocessing)

This process removes clear region and thin upper cloud area from whole range of Rapid Scan Observation and extracts detection target cloud.

Brightness temperature of IR1 is mainly used to filter out clear region. Pixels that have higher IR1 brightness temperature than a certain amount of threshold temperature are considered as clear region, and then the pixels are deselect from detection target. This method works for summer season which has high temperature near the ground surface.

Subtraction of IR1 and IR2 brightness temperature is utilized to clean up thin cirrus. This method is adopted for cloud type discrimination in general way, and use characteristics that IR1 brightness temperature of upper layer cloud consists of ice crystal is higher than IR2 brightness temperature of that because absorption of ice crystal at IR1 wavelength is smaller than absorption of ice crystal at IR2 wavelength (MSC/JMA 2000). On subtraction of IR1 and IR2, pixels exceed a certain amount of threshold are recognized as cirrus and these pixels are deselected.

In addition to above processes, comparatively optically thick cloud is extracted as detection target. In summer season, lower layer cloud basically consists of water droplets and number density of water droplets is large. This means lower layer cloud has large reflective power. Therefore, clouds which come up to condensation level and are in the growth process have large VIS reflectance. These clouds are detection targets. This process comes in taking clouds remained in cirrus discrimination process using former subtraction of IR1 and IR2 out of detection target. As well, VIS reflectance depends on solar zenith angle, observed value is divided by cosine of solar zenith angle. Processes use this corrected value. From this point forward, reflectance means this corrected reflectance.

Table 2.1 shows threshold used in preprocessing. Fig. 2.1 shows example of extracting detection candidate area (preprocessing). In Fig. 2.1, clear region, lower layer cloud area (possible fog) on Pacific Ocean and upper layer cloud area on East China Sea are removed.

Table 2.1 Elements and threshold used in the process of extracting detection candidate area (preprocessing).

IR1	288.15(K)	Filtering out clear region
VIS	0.45	Filtering out optically thin cloud extracting thick cloud
IR1 −IR2	2.0(K)	Filtering out thin upper layer cloud (cirrus)

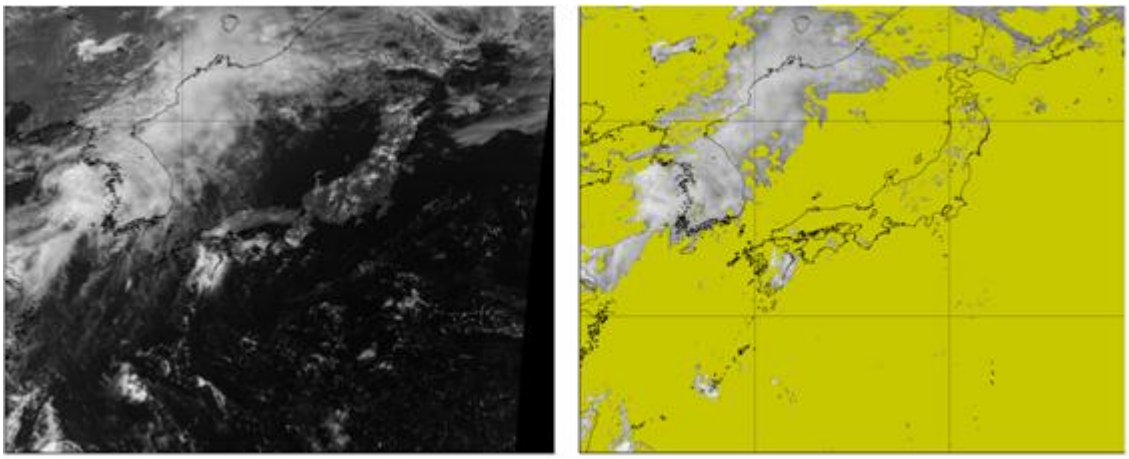

Fig. 2.1 VIS imagery (left) and preprocessed imagery (right) at 4:30 UTC July 13, 2011. Oak-yellow areas are removed by preprocessing.

2-2. Calculation Detection Parameters

In this process, explanatory variables (detection parameter) for detection are calculated by quantifying characteristics around the pixel which becomes detection target as a result of extracting detection candidate area process in the previous section. Table 2.2 shows parameter list for detection. In this parameter list, VIS reflectance (No. 1 in Table 2.2) and subtraction of IR1 and IR2 (No. 6 10.8 μm−12 μm in Table 2.2) are used to extract detection candidate area process. Detection parameters which have a correlation with phenomenon are used from these parameters in detection process. Compute process of each parameter except parameter No. 1 and No. 6 above mentioned are described below.

2-2-1. VIS Reflectance Maximum−Average in adjacent space (No. 2)

Purpose of this parameter is to acquire minute characteristics of cloud inside which develop to vertical direction in formative stage. When locally strong upward flow exists, reflective power becomes larger than that of around the cloud. As it turned out, value of this parameter is expected to enlarge.

Concretely speaking, among pixels become detection target, difference between maximum reflectance and average reflectance is obtained around the pixels. Average reflectance is calculated by only pixels which have reflectance value larger than threshold value of 0.45 in detection candidate area. Computing range of average reflectance (within 21×21 pixels) is different from that of maximum reflectance (within 7×7 pixels) as Fig. 2.2 indicates. Capturing local overshoot of cloud top is intended. Therefore this parameter might be negative at some pixels but these pixels are not adopted as available pixels in calculating prediction index and decision process at section 2-3.

Table 2.2 Detection parameter list (March 2012).

No.	parameters	Main objective
1	VIS	Detection of roughness which is observed at rising cloud top
2	VIS Maximum−Average in the adjacent space.	
3	VIS Standard Deviation in the adjacent space.	
4	IR1 Brightness Temperature Minimum−Average in the adjacent space.	
5	IR1 Brightness Temperature Standard Deviation in the adjacent space.	
6	Difference IR1−IR2	Rejection of thin cirrus (preprocess)
7	Difference IR3−IR1	Detection of water vapor above cloud top
8	Relationship of effective radius between IR1 brightness temperature and IR4 brightness temperature.	Presumptin of vertical structure about rapidly developing cloud.
9	Temporal variation of VIS maximum value in the adjacent space.	Presumption of developing level
10	Temporal variation of VIS average value in the adjacent space.	
11	Temporal variation of IR1 minimum value in adjacent space.	
12	Temporal variation of IR1 average value in adjacent space.	
13	Local drop of IR1 brightness temperature.	

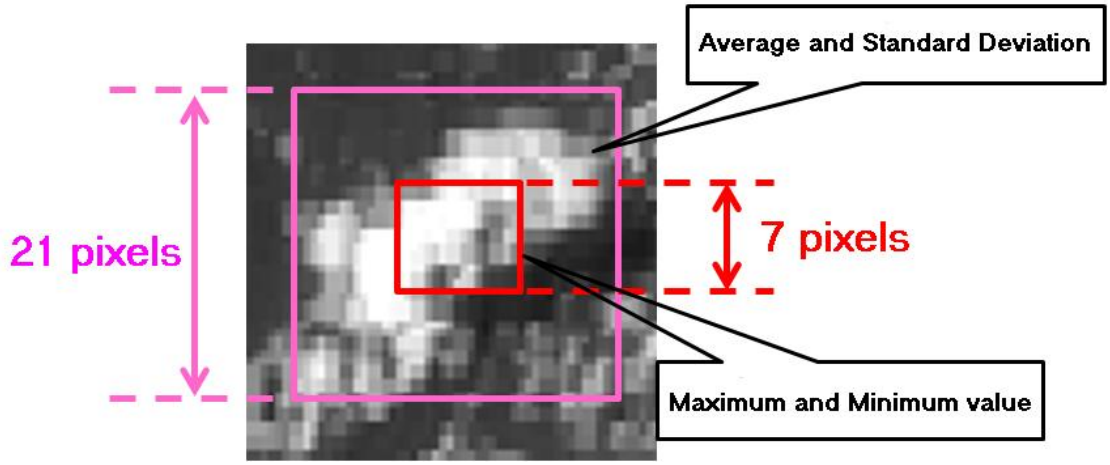

Fig. 2.2 Definition of the adjacent spaces

These spaces are used to obtain the maximum, average and standard deviation.

2-2-2. Standard Deviation of VIS reflectance in the adjacent space (No. 3)

Purpose of this parameter is to acquire cloud top asperity that becomes apparent as vertically developing cloud appears locally.

Standard deviation is calculated in range within 21×21 pixels which are detection target shown in Fig. 2.2. Standard deviation is calculated with pixels that VIS reflectance are larger than 0.45 as with subtraction of VIS reflectance maximum and average in the adjacent space, because clear region or thin upper layer cloud in the range makes standard deviation larger.

2-2-3. IR1 brightness temperature Minimum−Average in the adjacent space (No. 4)

IR1 brightness temperature approximately indicates the cloud top temperature on optically thick cloud as cumulus. Purpose of this parameter is to acquire minute characteristics in the cloud which is developing to vertical direction in formative stage. When locally strong upward flow exists, reflective power becomes larger than that of around the cloud. As it turned out, value of this parameter is expected to become large. The purpose is analogous to purpose of parameter No. 2. Resolution (VIS: 1–1.5km IR: 5–6km around Japan) makes characteristics of identical cloud on the screen different. This parameter, IR1 brightness temperature Minimum−Average in grid, is calculated just like parameter No. 2 to fill the gap.

Average is calculated within 21×21 pixels and minimum is calculated within 7×7 pixels which are detection target as Fig. 2.2 shows. Then parameter is obtained from both values. In case of this parameter become positive value along with parameter No. 2, the

pixel is not treated as available in later prediction index and decision process. The average is calculated by pixels which have smaller temperature than threshold (288.15K) used in extracting detection candidate area process because average becomes small in case clear region is in grid.

2-2-4. Standard Deviation of IR1 brightness temperature in the adjacent space (No. 5)

Purpose of this parameter is to acquire cloud top asperity that becomes apparent as vertically developing cloud appears locally. The purpose is analogous to parameter No. 3 difference of characteristics between VIS and IR is considered.

In detection target pixels, standard deviation is calculated using pixels smaller than 288.15K within 10 pixels for calculating average and standard deviation showed in Fig2.2.

2-2-5. IR differential 6.8 μm−10.8 μm (No. 7)

Because water vapor channel (6.8 μm: IR3) observes absorption band, radiation reaches satellite is emission from water vapor exists in middle or upper layer of atmosphere. For this reason, IR3 channel indicates the amount of the water vapor from upper layer to middle layer in atmosphere. The larger water vapor exists in upper or middle layer, the smaller IR3 brightness temperature become. Generally speaking, IR3 brightness temperature is smaller than IR1 brightness temperature because of absorption of water vapor. if cloud develops to tropopause, effect of water vapor between tropopause and cloud top. In this situation, IR1 and IR3 brightness temperature are almost equal. For that reason, difference of brightness temperature between IR3 and IR1 indicates altitude difference between tropopause and cloud top approximately. This difference of brightness temperature between IR1 and IR3 is expected to have comparatively large value from early phase to middle period of cloud development. This parameter is calculated by IR1 and IR3 brightness temperature of each pixel.

2-2-6. Relationship of effective radius calculated by IR1 and IR3 brightness temperature (No. 8)

According to Rosenfeld and Lensky (1998), radius variation of cloud particle from lower layer to upper layer is small compared to stratiform cloud that produces rain. Because strong upward flow, which rapidly developing cumulus cloud has, advects cloud particle to upper layer in short time. This means existence of super cooled water droplets in upper layer. Therefore radius of cloud particle near cloud top is expected comparatively small. There is a chance to be able to separate between rapidly developing cumulus

cloud and others by estimating quantitatively and parameterizing its characteristics. Thus purpose of this parameter is to estimate vertical cloud structure from relationship between effective radius of cloud particle and IR1 brightness temperature in a certain range.

IR4 (3.8 μm) that is near infrared channel is used to calculate effective radius. IR4 channel observes both solar radiation and infrared radiation from earth in daytime. And solar radiance is influenced by radius of cloud particle near cloud top. According to Nakajima and King (1990), effective radius is determined by only solar radiance of 3.7 μm in optically thick cloud. Infrared radiation from cloud top estimated by IR1 brightness temperature is subtracted from observed radiation of IR4 to extract solar radiance component. Then effective radius of cloud particle is obtained by the solar radiance component.

Observed radiance $L_{3.8}$ of IR4 channel is given by equation (1).

$$L_{3.8} = t_{3.8}^{0}\left(\frac{F_0\mu_0}{\pi}\right)\rho_{3.8} + t_{3.8}^{'}B_{3.8}(T)(1-\rho_{3.8}) \qquad (1)$$

F_0 is solar radiance flux on 3.8 μm band, μ_0 is cosine of solar zenith angle, $B_{3.8}$ is Plank function, $\rho_{3.8}$ is reflectance on 3.8 μm band, $t_{3.8}^{0}$ is transmittance in reflective channel of solar radiance, $t_{3.8}'$ is transmittance of radiance from cloud top, T is cloud top temperature. Radiance $L_{10.8}$ of 10.8 μm band (IR1) in dry atmosphere is given by the next equation (2).

$$L_{10.8} = t_{10.8}^{'}B_{10.8}(T) \qquad (2)$$

Along with Rosenfeld and Lensky (1998), $t_{3.8}' = t_{10.8}' = 1$, $t_{3.8}^{0} = 0.75$ would be assumed, and $\rho_{3.8}$ is obtained from (1) and (2). According to Kaufman and Nakajima (1993), relation between effective radius and reflectance is empirically given by approximate curve below.

$$\ln(\rho_{3.8}) = a_0 + a_1 r_e + a_2 r_e^{\,2} + a_3 r_e^{\,3} \qquad (3)$$

Here, $a_0 = -0.68460$, $a_1 = -0.08243$, $a_2 = -0.00749$, $a_3 = 0.00033$. Oku and Ishizuka (2008) calculate effective radius using IR4 channel of MTSAT-1R by this method and confirm validity of the result on mid-latitude of north hemisphere. However maximum value of effective radius obtained by this method is about 20 μm.

Okabe et al. (2011) defined “slope index” below which showed relationship of IR1 brightness temperature and effective radius by considering pixels within 10 pixels around target pixels as one cluster. The slope index is adopted as Parameter No.8.

$$slopeindex = \arctan\left(\frac{\sqrt{\sum_{i=1}\sum_{j=1}\left(TB_{10.8(i,j)} - \overline{TB_{10.8}}\right)^2}}{\sqrt{\sum_{i=1}\sum_{j=1}\left(R_{e(i,j)} - \overline{R_e}\right)^2}}\right) \quad (4)$$

This slope index corresponds to gradient in coordinate configured vertical axis as brightness temperature and horizontal axis as effective radius. The bigger parameter is, the smaller change of cloud particle radius along vertical direction compared to change of brightness temperature. In this case, strong upward flow is expected.

Effective radius calculation is not necessarily performed for all pixels become detection target. Reasons are below.

・Calculation method of effective radius is limited to lower layer cloud (Oku et.al. 2008).

・Dependence of solar zenith angle exists.

For this reason dealing with this parameter is required attention as discussed in section 2-3 about handling as of March 2012.

2-2-7. Time trend of VIS Average and Maximum in Grid (No.9, No.10)

From here, feature amount change of short duration by Rapid Scan Observation is parameterized. Variation of average and maximum in grid five minutes interval is obtained in area showed in Fig 2.2. Increase of optical thickness as cloud growth is detected by finding out time variation of VIS.

Location correction is necessary for cloud motion to evaluate time variation adequately. Therefore, displacement is calculated by inter-correlation method using observation image for detection and previous observation image. This displacement calculation method is basically similar to Atmospheric Motion Vector (AMV) (Shimoji et.al. 2010) (discussed later in section 2-2-9). However, Dependence of solar zenith angle occurs by using VIS image, normalized correction for detection image and previous image is performed by only cosine of solar zenith angle because 5 minutes interval is short.

Time variation of average value in grid is calculated by subtracted each pixels of detection image and previous image before average process is performed (Fig 2.3). To average difference of all pixels is identical with obtaining difference between average of detection image and its previous image. At equation (5), Grid B stands for detection grid and Grid A stands for previous grid.

$$Average\_VISmean = \frac{1}{N}\sum_{i}^{21}\sum_{j}^{21}\{GridB(i,j) - GridA(i,j)\} \qquad (5)$$

This process is able to perform in case of obtaining back to back two images at five minute interval. However MTSAT-1R observes Northern Hemisphere in order to ensure image position accuracy at two hours interval. Consequently, the process is executed by using combination of small domain observation with Northern Hemisphere observation. In this case, time interval of Japanese domain the product uses is non-constant because the observation method between small domain observation and Northern Hemisphere observation is different. The time interval is 7.8 minutes in case of combination small domain and Northern Hemisphere observation. As it turned out, the process deals with variation for 7.8 minutes in this case. The variation for 7.8 minutes is converted to variation for 5 minutes in this process. In concrete terms, variation for 7.8 minutes is divided by conversion coefficient 1.56 (=7.8/5). However, time variation of phenomenon is assumed as linear.

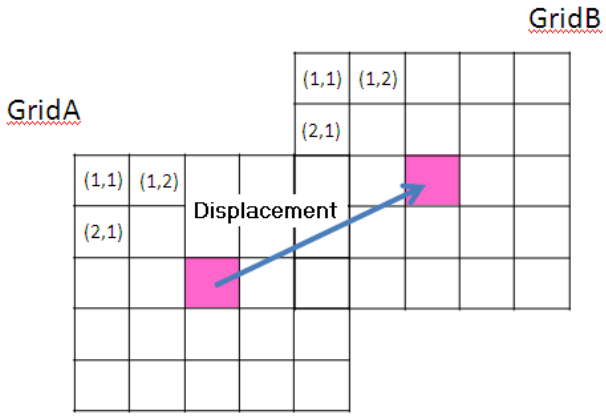

$$Timediff(i,j) = GridB(i,j) - GridA(i,j)$$

$$Average\_VISmean = \frac{1}{N}\sum_{i,j} Timediff(i,j)$$

Fig 2.3 Average in Grid

2-2-8. Time Variation of Minimum brightness temperature (No.11) and Average brightness temperature (No. 12) of 10.8 μm in Grid

Time Variation of maximum and average brightness temperature in Grid described at Fig2.2 for five minutes is obtained. Purpose of these parameters is to evaluate rise of cloud top altitude by obtaining time variation of 10.8 μm brightness temperature.

Calculate method is same as time variation parameter of VIS (2-2-7).

2-2-9. Localized drop in 10.8 μm brightness temperature（No. 13）

This parameter is defined as a value of subtraction 10.8 μm minimum value of time difference in Grid from 10.8 μm average value of time difference in Grid. Purpose of this parameter is to complement detection capability of cumulus cloud developing trend by evaluating localized cloud top rising unless climb up trend of cloud top in Grids scale (No.12) is obtained.

2-2-10. Motion Cancelation

As stated above, displacement vector is calculated by inter-correlation method over all pixels become detection target in extracting process of detection candidate area in order, consequently this is used for calculating time difference parameter. Besides this, IR1 imagery transformed to 0.04 degree lattice coordinate is used because of computer resource. There are two definitions below about tracking process for motion cancellation.

I. Template: Area is to define characteristics of cloud for tracking it on imagery.

II. Search area: Area is to search conformable cloud using the template.

Template size described in I. is 5 square pixels in product as of March 2012. As a matter of fact, this means cloud characteristics included in 0.2 square degrees (about 20 square km) is used for tracking process. But the optimum template size may be different for phenomena scales to track.

II stands for a range which is able to calculate displacement. This process uses 7 square pixels as of March 2012. This means displacement of 0.12 degree maximum is available for tracking. It can track displacement of cloud moving at 40m/s near Japan. The reasons why the product uses 7 square pixels are main target is to track cumulus cloud as typified by Heat lightening developing in comparatively small wind speed environment from lower layer to middle layer and computation time tradeoff. On the other hand, the size of search area is not enough near jet stream like frontal zone. Consequently, the tracking process is not able to calculate accurate displacement or has possibilities of delivering maximum value limited by this process. In addition to this, case of small range and Northern hemisphere observation described in section 2-2-9 takes expand of time interval into account, and then the tracking process uses 11 square pixels expanded search area multiplied by 1.56 (=7.8/5) to calculate cloud displacement. Then comparison and searching the position of high degree of similarity in search area are executed by using characteristics of template included in search area. Consequently, the position that has large similarity index is adopted as displacement of cloud between two imageries. This process uses correlation coefficient as criteria to judge the similarity.

This means high degree of similarity is large correlation coefficient and the maximum correlation coefficient (simply called correlation coefficient afterward) derived with displacement can be used as reliability of cloud displacement. This method could not properly track developing cumulus cloud or cumulus nimbus cloud which changes enormously in short time because small change of cloud shape is premised in this method. Besides this, there is limitation which is not enough to track clouds in large wind speed area discussed before. On these accounts, displacement of each pixel does not adopt calculated result of each pixel directly but smoothing result derived from vectors of surrounding pixels that has large correlation coefficient. The smoothing method employed as of March 2012 is stated below.

I. Pixel has correlation coefficient of 0.7 larger and is detection target in detection process of candidate area becomes valid pixel for tracking process. Pixel is 0.01 degree square grid unit.

II. When number of valid pixel for tracking process exceeds 10% of 11 square pixels around detection target pixel, displacement vector of these valid pixels for tracking process is averaged in unit vector. It is displacement of target pixel.

III. If number of valid pixel for tracking process is smaller than 10% of 11 square pixels, pixel is not used in detection process, because accurate displacement cannot be calculated.

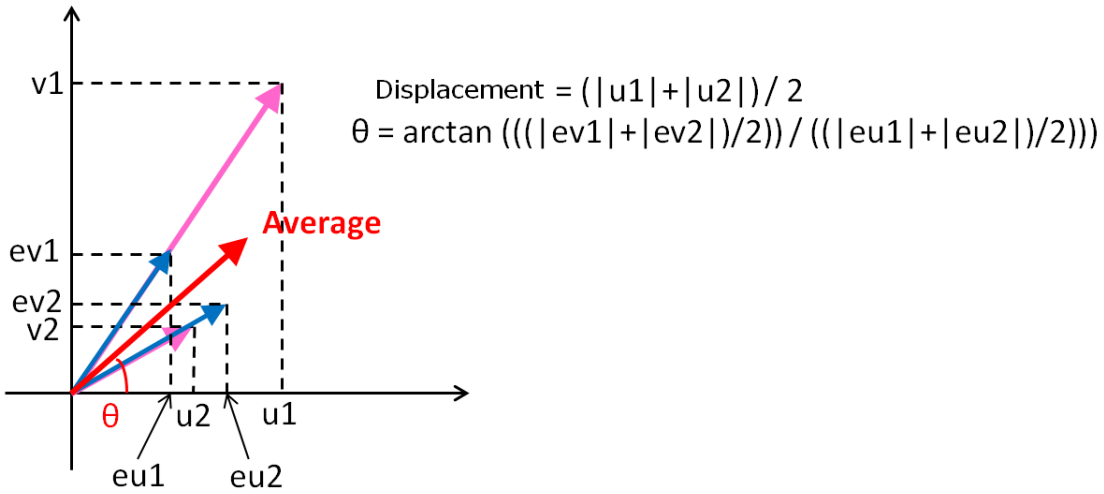

Fig2.4 Average in unit vector for smoothing displacement (In case of 2 vector)

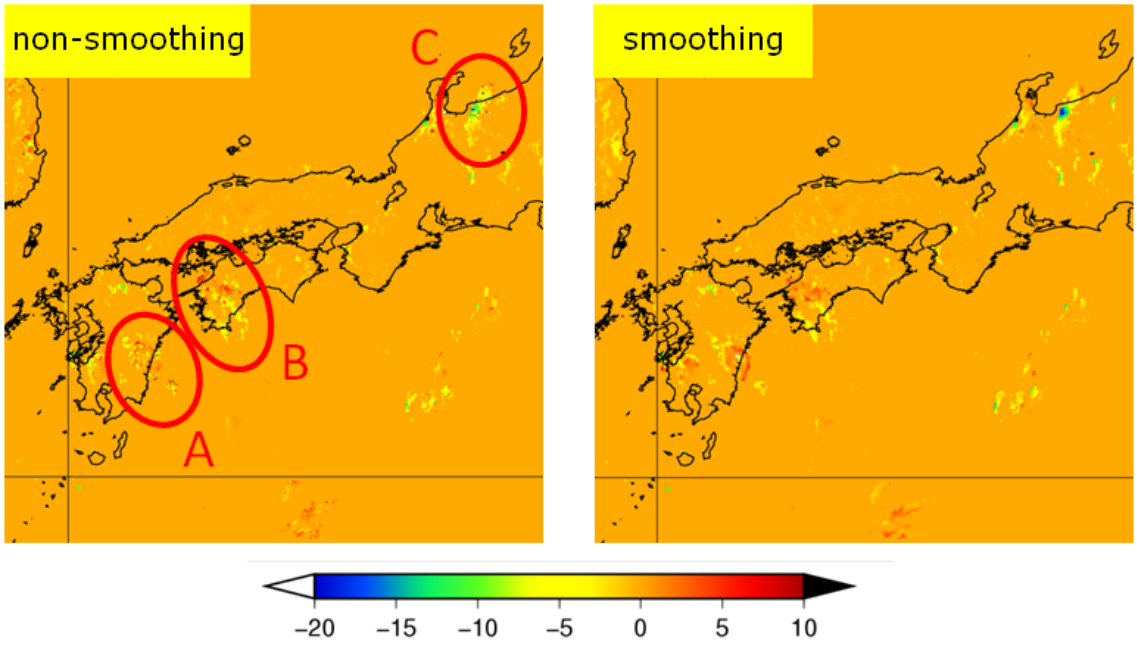

Fig 2.5 Difference of parameter No.12 motion cancellation process applied. Left image shows result of non-smoothing and right image shows result which smoothing process applied.

Fig2.4 shows example of average in unit vector described above II in case of 2 vector average. In this case, moving direction does not depend on length of each vectors, consequently smoothed vector has a meaning of “most probable moving direction”.

Fig2.5 is distribution maps show results of non-smoothing and smoothing applied to parameter No.12 which is time variable parameter of IR1 brightness temperature. In Fig2.5, Areas of A, B and C are convective cloud area. Areas of A and B have comparatively large difference between increased temperature part and decreased temperature part in each cloud areas in smoothing case compared to non-smoothing case. Hence these area is distinguished clearly. And in area C, decreased temperature part is specifically calculated in smoothing case compared to non-smoothing case.

2-2-11. Solar Zenith Angle Correction of VIS parameter

Fig2.6 and Fig2.7 shows reflectance difference by solar zenith angle on observed imagery of frontal cloud band which consists of upper or middle level cloud. Frontal cloud band is selected because it is comparatively large spatial scale and has little time variation. VIS parameter No2 and NO3 depend largely on solar zenith angle from these result. Then relationship between the parameters and solar zenith angle is empirically obtained by some cases which seem little time variation of structure and correction is executed. Correction method is described below.

I. Dependence between the parameters and solar zenith angle is obtained. Sample data is cutout area from large scale precipitation system. Dates are 3, 17 in July, 20, 21, 28 in August, and September 5 2011.

II. Range of solar zenith angle is separated into 200 bins and each bin include same number of samples. Average and standard deviation (sigma) are calculated from each bin.

III. Average of each bin is calculated again using samples included in value of average obtained. Solar zenith angle of each bin uses value intermediate of each bin.

IV. Regression expression is obtained by regression analysis of quadratic function.

V. The parameters which solar zenith angle is over 30 degree are corrected by the regression expression.

Fig2.6 and Fig2.7 shows dependence of solar zenith angle and correction result about parameter No.2 and No.3. Table2.3 shows coefficient of regression expression for correction. As a result, the parameters are considered to be calculated without effect of solar zenith angle up to 75 degree against constant structure target like frontal cloud band. Consequently, Range that VIS parameter is available is limited under 75 degree.

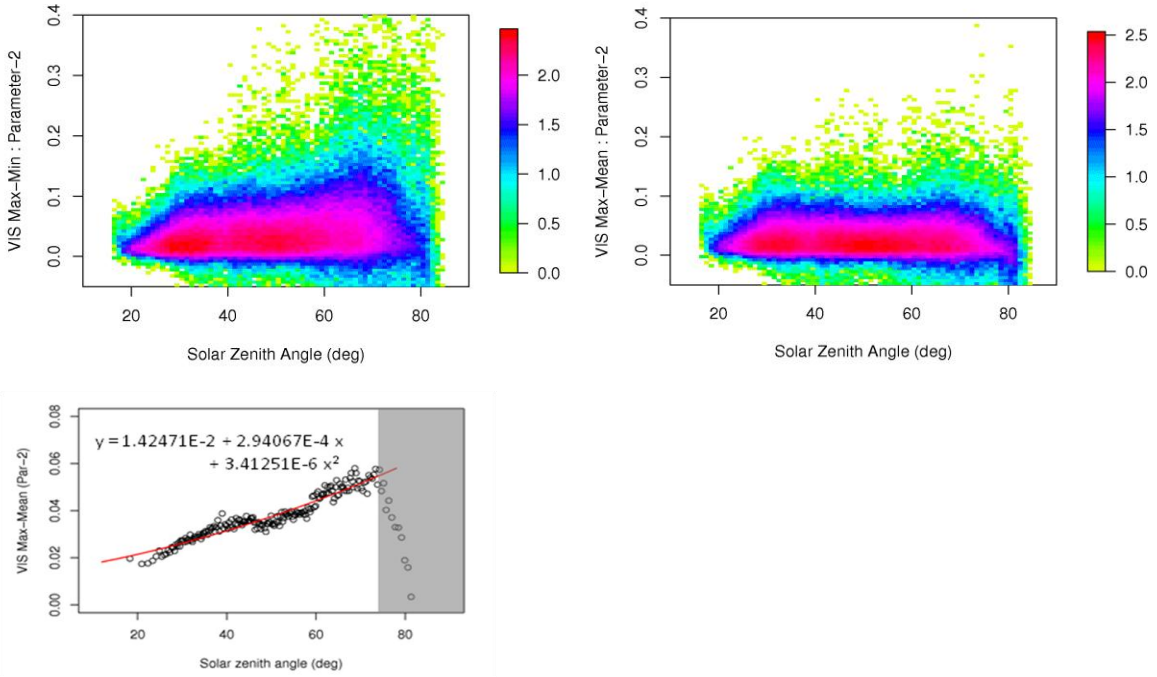

Fig2.6 Correction of parameter No.2 using solar zenith angle
(Upper left) dependence of solar zenith angle before correction
(Upper right) dependence of solar zenith angle after correction
(Lower left) correction data and it's quadratic approximation curve
Color scale shows common logarithm of number of samples.

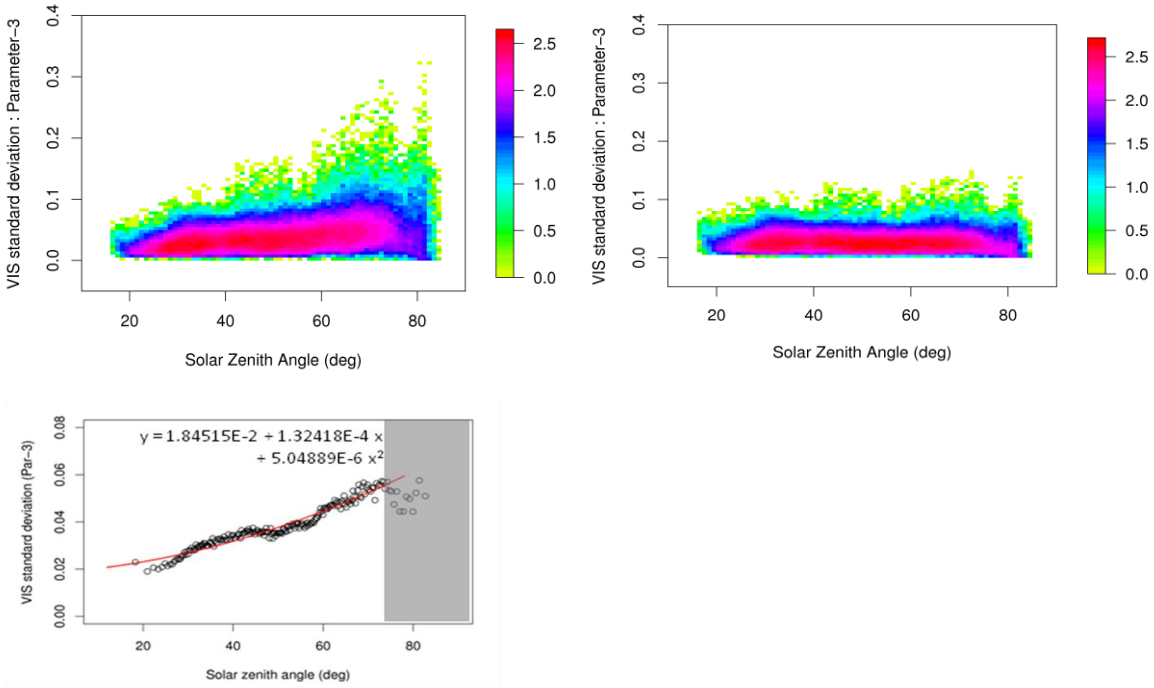

Fig2.7 Correction of parameter No.3 using solar zenith angle
(Upper left) dependence of solar zenith angle before correction
(Upper right) dependence of solar zenith angle after correction
(Lower left) correction data and it's quadratic approximation curve.
Color scale shows common logarithm of number of samples.

Table2.3 Coefficient of quadric equation y= intercept + Ax + Bx^2
This approximation expression is to correct parameter No.2 and No.3 for solar zenith angle (as of March 2012).

Parameter	Intercept	Coefficient A	Coefficient B
No.2	0.0142471	2.94067E-4	3.41251E-6
No.3	0.0184515	1.32418E-4	5.04889E-6

2-2-12. Dealing with each parameter of pixels become detection target

Kind of parameters brought in as of March 2012 and calculation method has been described up to here. Parameters are not calculated or dealt with invalid value when condition is not met conditions. Table2.4 shows calculation condition of each parameter and its handling. In practice, parameters which are available from sensitivity evaluation described next section are used in calculation of prediction index and screening process of cloud development.

Table2.4 Calculate condition and handling of detection parameter

Parameter No	Condition to calculate	Handling when not meet condition
2	7x7 maximum >= 21x21 average	Not use in screening process
3	–	–
4	7x7 maximum >= 21x21 average	Not use in screening process
5	–	–
7	–	–
8	Pixels which meet conditions below exist in 21x21 pixels. 1.IR1 brightness temperature is over 250K 2.Solar radiance is proper value to obtain effective radius of IR4. 3.When effective radius is on the abscissa and a IR1 brightness temperature value on the ordinate, slope is positive value.	-999 is error value. Not use in screeing
9	Ratio of available tracking pixels included around 11 square pixels is greater than 10%.	-999 is error value. Not use in screeing
10		
11		
12		
13		

2-3. Calculation prediction index and screening process

Prediction index to use screening process is calculated by using detection parameters described former section. Some sort of criteria is necessary to evaluate presence of phenomenon. Location data of lightening observation system (LIDEN) which JMA operates is used as truth data in this product. That is to say all cumulus or cumulus nimbus cloud is assumed to have lightening after Rapidly Developed. Both of anti-surface and inter-cloud discharges are used from LIDEN data. Strictly speaking,

center of developed convective cell does not spatially match up precisely with discharge distribution and there are also errors in LIDEN observation. Therefore, use of large number of samples intends to diminish effect of these error factors. However, target area is limited around Japan where LIDEN data exist.

2-3-1. Sensitivity evaluation of detection parameters

Parameter sensitivity assessment is performed by method stated below in order to evaluate sensitivity against lightening. Consequently, event probability against each parameter is obtained.

1. Pixels that become detection target in extracting detection candidate area and are able to be calculated become parent population of each parameter over a period of time.
2. These parent populations of each parameter are stratified by IR1 brightness temperature, and then they become parent population of each parameter and each temperature. Stratification is 3 classes. First is smaller than 250K, second is equal or larger than 250K and smaller than 273.15K, third is equal or lager than 273.15K and smaller than 288.15K.
3. Each parent population is equally parted into some bins. Rate of lightening case which began within 60 minutes of observation start is obtained from each bin.
4. Lightening observation of each sample is investigated by tracking cloud during 60 minutes which considered cloud moving. Tracking process is performed as similar as motion cancelation described in section 2-2-10.
5. Then lightening is checked whether it is observed or not within 0.1 degree (about 10km square around Japan) of migration path which is derived from tracking process noted above.

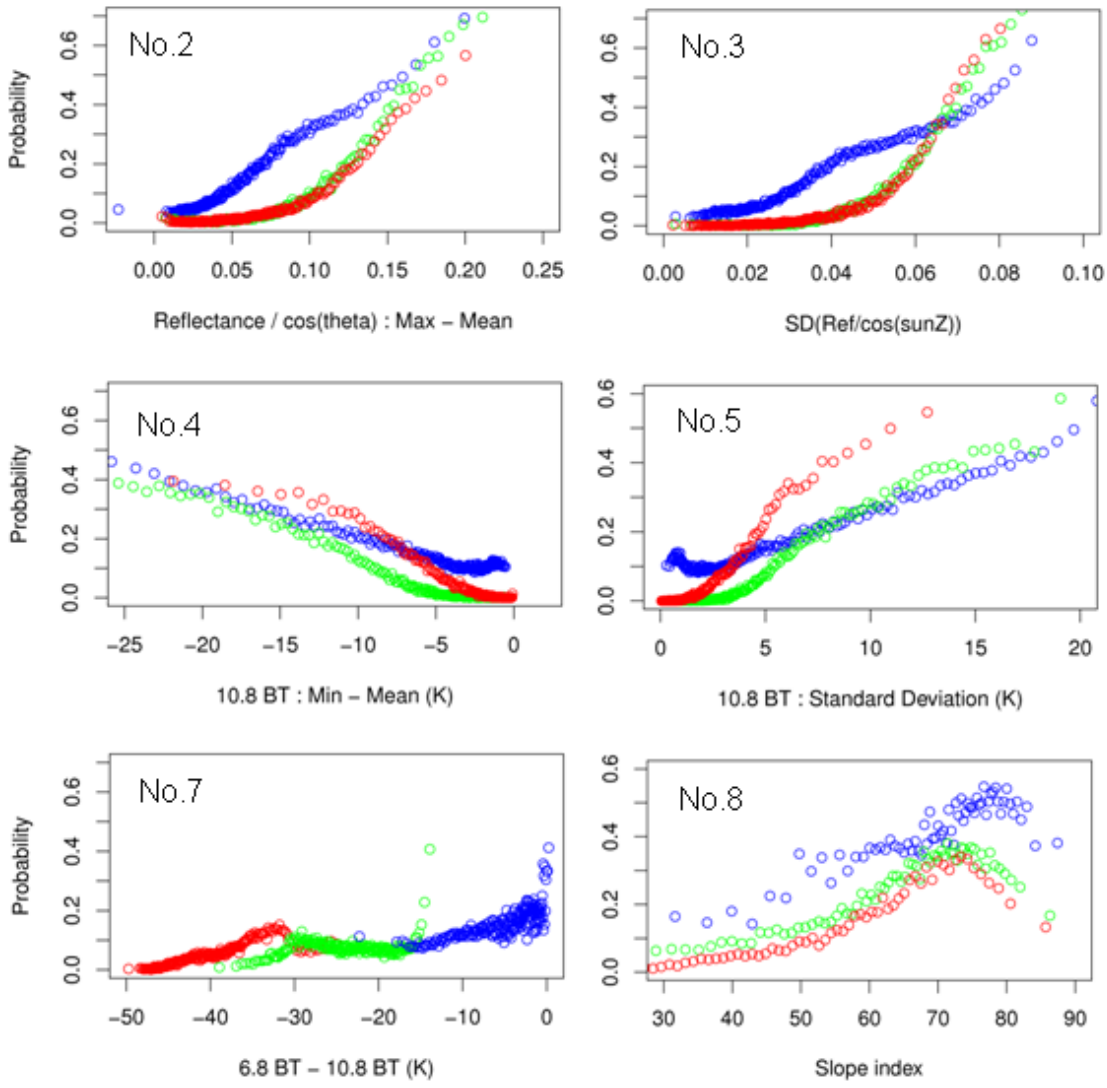

Fig2.8 Sensitivity assessment of each parameter (No.2 to No.5, No.7, No.8)
Red:273.15K to 288.15K, Green:250K to 273.15K, Blue: up to 250K

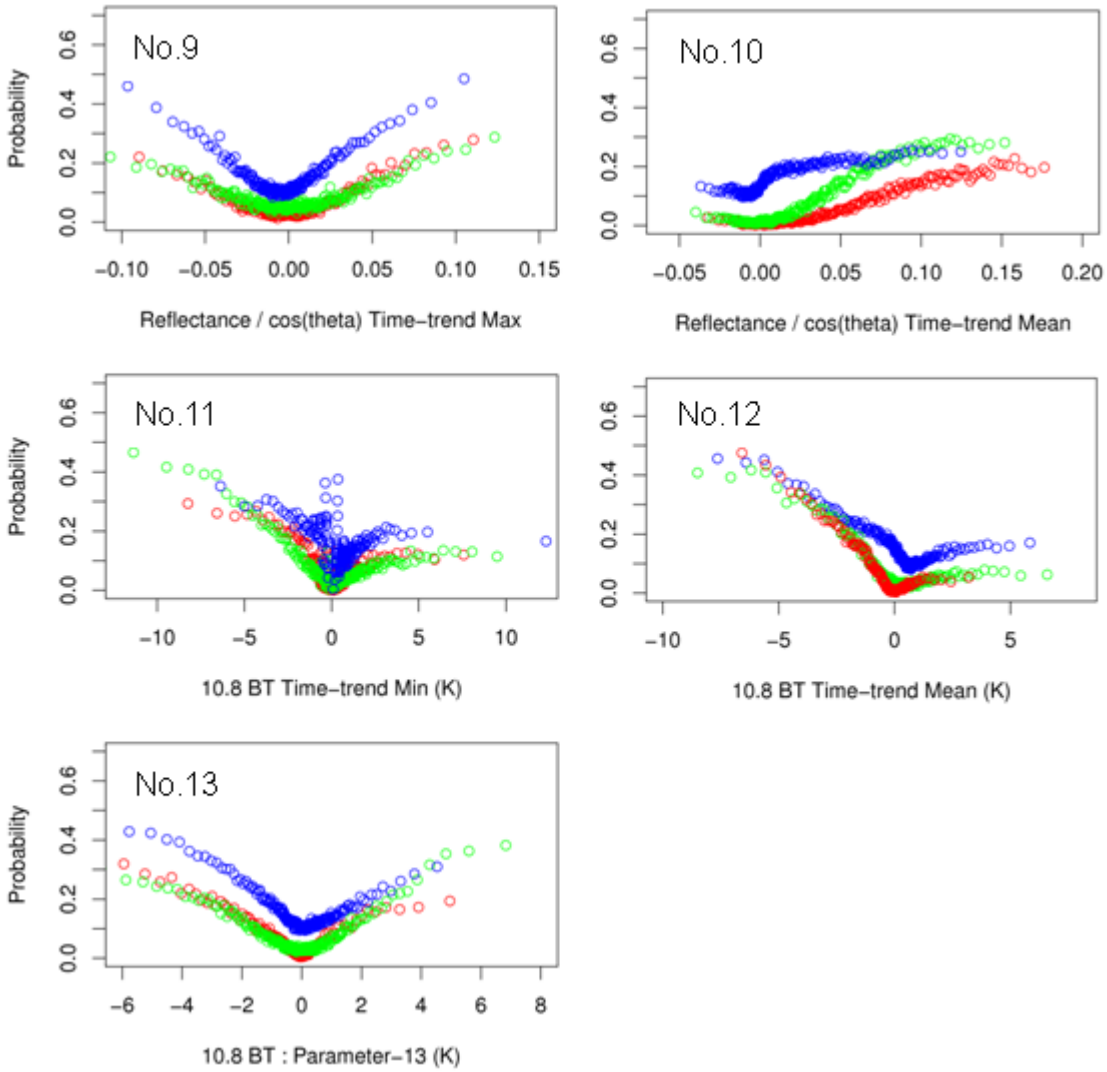

Fig2.9 Sensitivity assessment of each parameter (No.9 to No.13)
Red: 273.15K to 288.15K Green: 250K to 273.15K Blue: up to 250K

In this product, evaluation is executed using heat lightening which is main detection target. Fig2.8 and Fig2.9 show result derived from data are from 03:00UTC to 07:55UTC of July 10 to July 13 in 2011. Fig2.8 (time static parameter) shows that parameter No.2 to No.5 have good correlation with lightening rate however parameter No.7 doesn't have correlation with it. Parameter No.8 is not monotone increasing and has a peak at 70. Time variation parameter No.10 has positive correlation with lightening rate, while parameter No.12 has negative correlation with lightening rate in Fig2.9 (time variation parameter). These indicate that there is correlation between

development of cloud and lightening rate. Meanwhile other parameters are symmetric distribution around 0. For example, parameter No.9 indicates a certain level of lightening rate at lower reflectance. These causes are considered that accuracy of motion cancelation described in 2-2-10 is not enough and maximum value (or minimal value) of different pixel as time variation parameter in Grid is captured on the way of tracking process.

In the result, parameter No.2, No.3, No.4, No.5, No.10 and No.12 are adopted as sensitive to lightening phenomenon. They are almost monotone increasing or decreasing parameters. Positive range of No.2, No.3, No.4, No.5 and No.10 is used and negative range of No.12 is used in this regard. Then next prediction index is calculated. Condition of calculation of prediction index is all explanatory variables are calculated. Pixel that the condition is met and prediction index is calculated is valid determinable pixel.

2-3-2. Prediction index by logistic regression

Logistic regression analysis is performed using adopted parameters. Logistic regression analysis is one of non-linear multiple regression analysis. This analysis is often used when binary statistical result like 0 or 1 is required. This product also requires result of detection or not detection, then logistic regression analysis is better suited. Multiple regression model is given by equation (6).

$$p = \frac{1}{1+\exp\left\{-\left(a_0 + \sum_i a_i x_i\right)\right\}} \tag{6}$$

Dependent variable p indicates probability of detection and $0 \leqq p \leqq 1$. If lightening is predicted, p is 1. Explanatory variables x is parameter described in previous section and a is constant or coefficient to the parameter. They are called regression coefficient in what follows.

Regression coefficients of each temperature zone are calculated using parameter as explanatory variable in previous section and LIDEN positioning data. Three points are considered below in carrying out regression analysis.

1. a lot of cases are picked up in order to converge.
2. In case that coefficient which is obtained by regression analysis shows converse against the trend obtained in section 2-3-1, this parameter is not used in the temperature zone.
3. Parameter No.2 and No.3 is adjusted to be linear relationship between parameter value and lightening rate by equation (7) below (Fig2.10).

$$corrected\_param = \exp\left(param^2\right) - 1 \qquad (7)$$

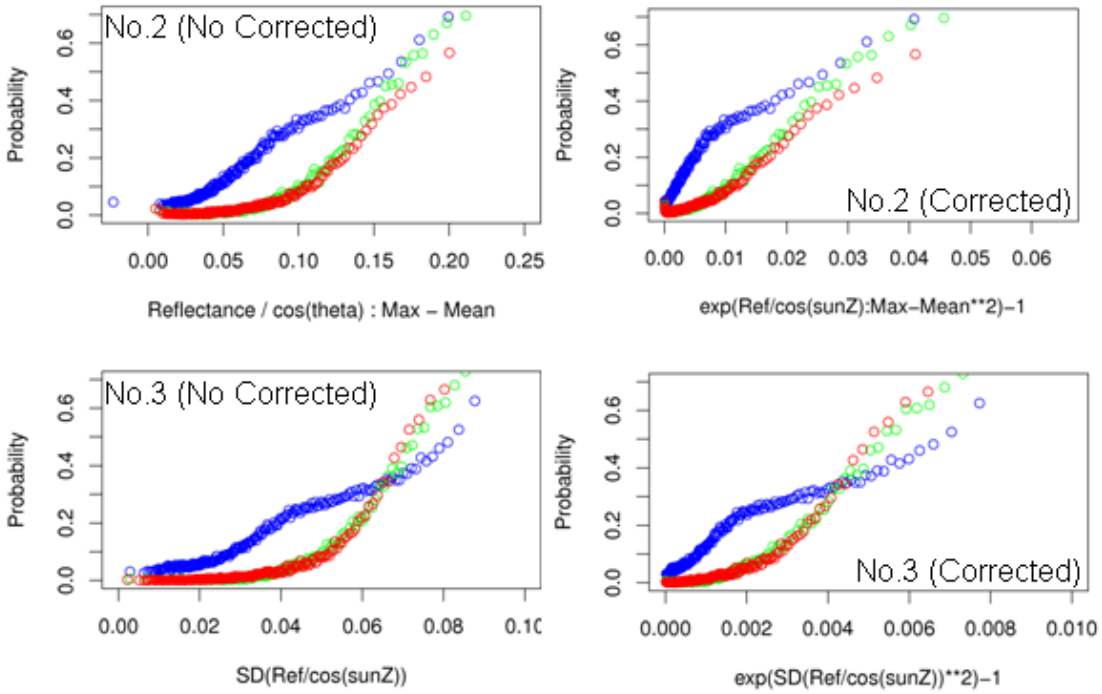

Fig2.10 Parameter Correction in logistic regression analysis (No.2, No.3)

Correction equation : exp(parameter^2)-1

Table2.5 List of Explanatory variable and coefficient

***** means parameter is not used as explanatory parameter.

Expanatory Variable	～250K	250K～273.15K	273.15K～288.15K
constant	－2.237879	－5.051168	－5.724653
exp(No.2^2)-1	49.771237	54.370960	31.462799
exp(No.3^2)-1	177.862775	377.402861	443.293052
No.4	*****	－0.017522	*****
No.5	0.021747	0.058799	0.176924
No.10	*****	9.473337	10.908360
No.12	－0.061127	－0.053739	－0.195936

Table 2.5 shows parameters and coefficients calculated in logistic regression. Lightening dominant case which is 03:00UTC to 07:55UTC in 10 to 13 July 2011 is used in logistic regression. This is following reason.

I. Enhance detection sensitivity to heat lightening which is difficult to forecast.

II. Ensure lead time.

I. is concerned that detection accuracy of developing cloud in large scale disturbance, for instance frontal zone, drops to lower value the result of having strong sensitivity to heat lightening and then error detection for lower level cumulus cloud or upper layer cloud area will occur. In similar way, Ensuring lead time and increasing error detection are competing in II. Though tuning method for heat lightening is selected as a trade-off for some error detection.

Fig2.11 shows relation between probability based on logistic regression and actual phenomenon occurring rate. Three cases which are independent to regression analysis cases are picked up. First is heat lightening case in high-pressure system over Pacific Ocean in July 9 2011. Second is unsteadiness precipitation case which has lightening by cold trough in July 26 2011. Third is weak ridge case which is back side of cold trough in July 29 2011. Forecasted probability and actual phenomenon is comparatively agreed on heat lightening and unsteadiness precipitation with lightening phenomenon, probability by this method holds account for potential of phenomenon occurrence. However, case of July 29 in 2011 shows too much or undervalued probability, former is missed and later is passed. The reason why is that heat lightening case is adopted for tuning and unsteadiness of atmosphere is not used as explanatory variable. The former problem brings further optimization for tuning method and the later problem has room for improvement bringing in other observation or forecast data to figure out atmospheric vertical structure which is difficult to be observed by geostationary meteorological satellite.

Practically, index from logistic regression is corrected by empirical coefficient according to rank of temperature. As of March 2012, correction coefficients are 0.429 which is smaller than 250K, 0.60 which is equal or greater than 250K and smaller than 273.15K, and 1.0 which is greater than 273.15K. This is following reason.

I. Prevent detection accuracy dropping to lower value because of optically thick cloud, detection candidate area extracting process is not able to weed out, for example middle layer cloud of altocumulus or altostratus, and multi layer cloud of combination of lower and upper layer cloud

II. Give increased Priority to lower layer cloud in early developing which is main target of this product.

This prediction index is used in latter part of determining process.

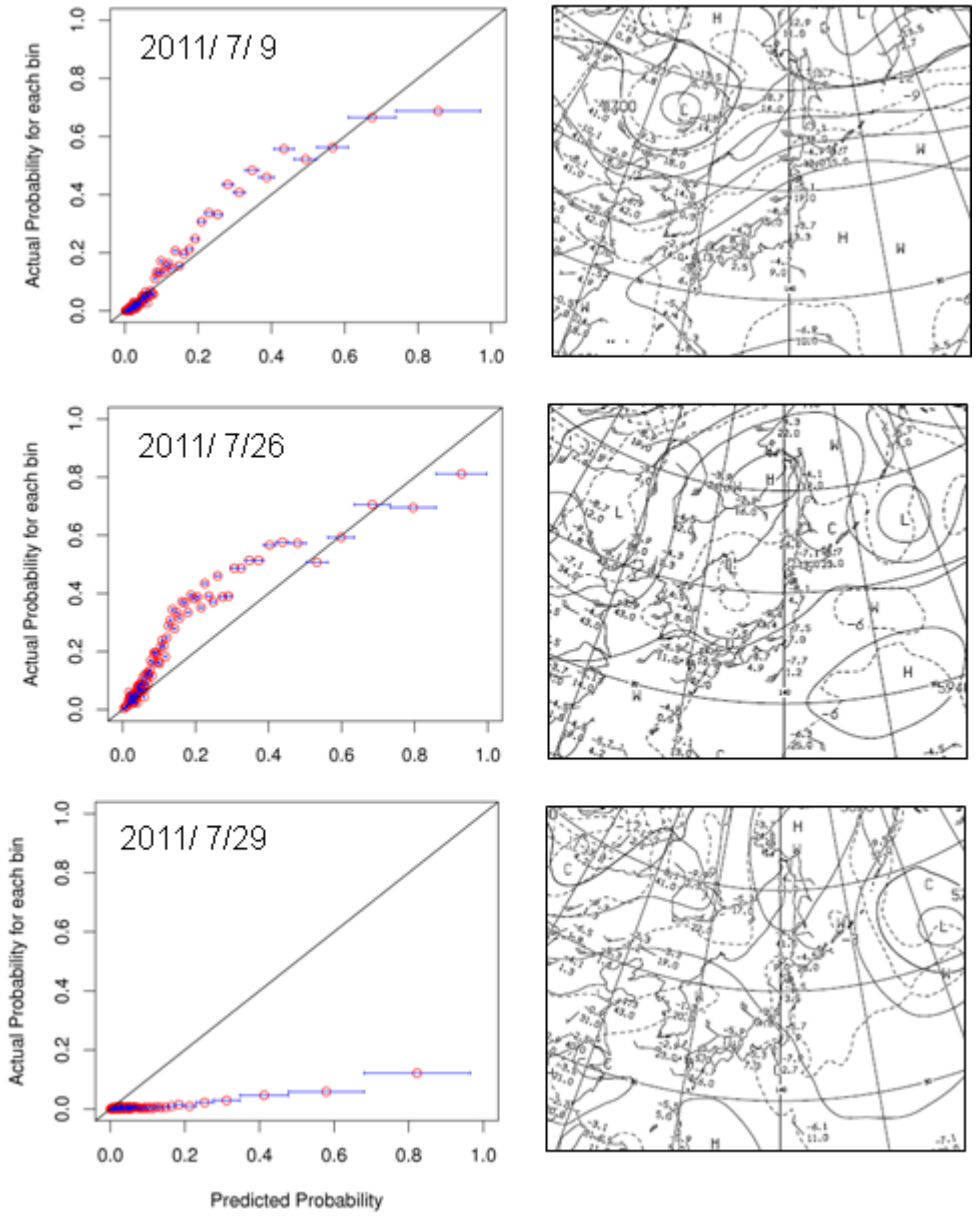

Fig2.11 Relation between probability of logistic regression (right columns) and actual lightening rate (left column).
Weather charts at 500hPa on 0:00UTC (right column).

2-3-3. Decision process

Prediction index is calculated in pixel unit of 0.01 degree grid, though resolution of observed IR imagery is about 0.05 degree around Japan for real, and position is low-accurate when parameters of motion cancelation etc are calculated. Therefore, the index is calculated in 0.1 degree unit and a grid including 10 square pixels is defined for 0.1 degree unit. Valid determinable pixel has been described in section 2-3-1. Fig2.12 shows flow of the decision process.

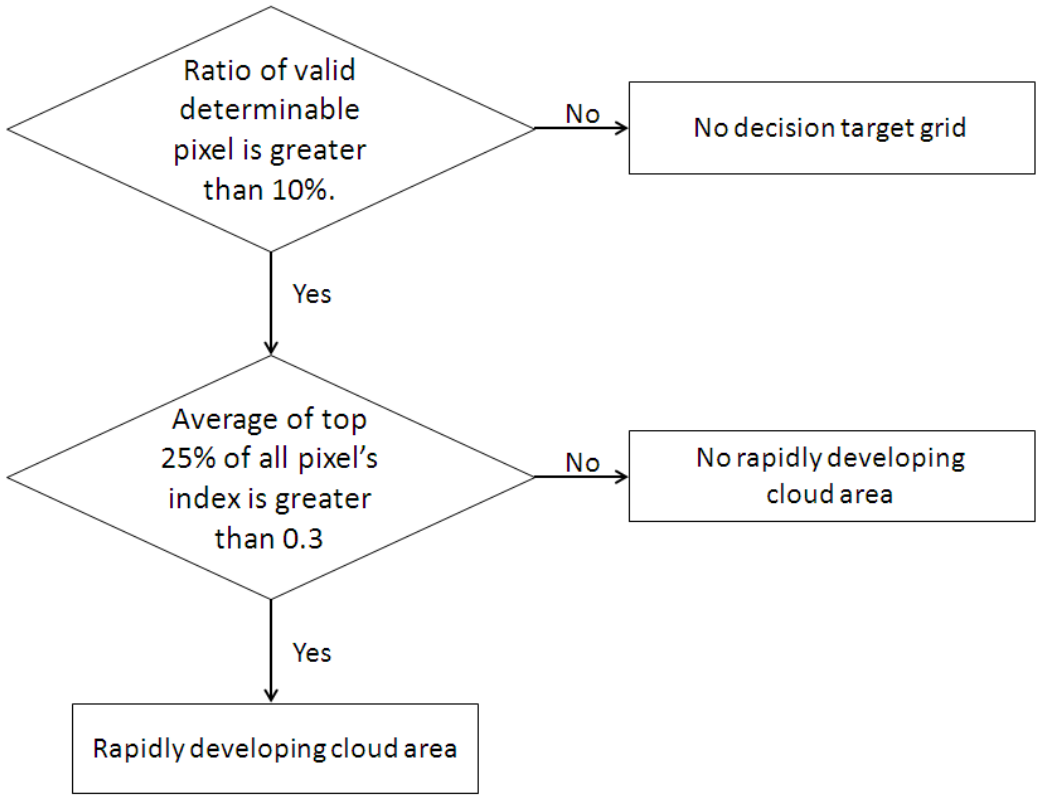

Fig2.12 Flow of decision process

Grid is 10 square pixels unit described in 2-3-3.

3. Detection case of rapidly developing cloud area and scores

3-1. Detection case of rapidly developing cloud area

Actual detection cases based on the method described previous paragraph and characteristics of algorithm as of March 2012 are overviewed. Image of rapidly developing cloud area detection is different from image of cumulus nimbus cloud information product.

3-1-1. Case of heat lightening (July 14 2011)

Fig3.1 shows case of heat lightening observed in July 14 2011. Green painted parts of upper left image indicate detected rapidly developing cloud area. Precipitation echo was observed at A, B and C in figure but developing trend was not clear. They developed to have lightening 20 or 30 minutes later. Rapidly developing area was detected in a part of line of cumulus cloud in Japan Sea and its echo got up strong while lightening was not detected. This case shows that this product can be helpful information whether cumulus cloud rapidly develop or not in area without upper layer cloud under high pressure system. A combination of this product and other information indicates atmospheric instability will increase Capability of shot time forecast for rapidly developing cumulus cloud.

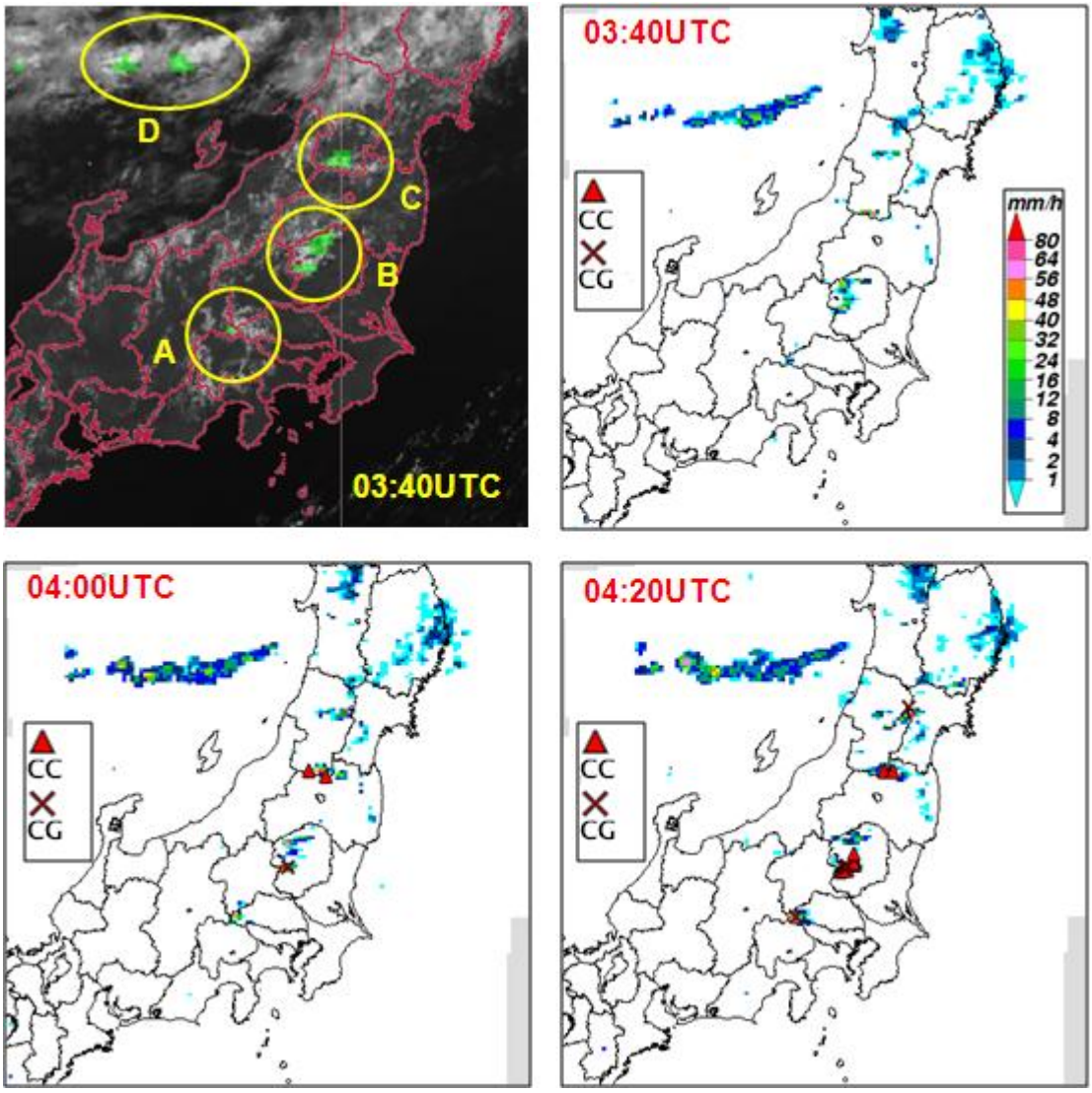

Fig3.1 Case of heat lightening (03:40UTC July 14 2011)

3-1-2. Case of heavy rain with lightening when front go southward. (Aug 26 2011)

Fig3.2 shows detection case in Aug 26 2011. Front went southward to southern shore from daytime to evening and short time heavy rain with strong lightening in wide area was observed. At 4:40UTC of detection time, surface front existed on inland area and lightening was already observed. Clouds near frontal zone were detected as rapidly developing cloud area and active lightening continued after that. Cumulus clouds (A, B and C in figure) which were generated on lower layer convergence line in warm side of frontal zone developed to have lightening after detection of this product. Detected area is wide to a certain degree because determination is executed by 0.1 degree grid unit noted in section 2-3-3. There are areas which are seem to be error detection in terms of each cumulus cloud scale, however trend of cloud development was well figured out totally.

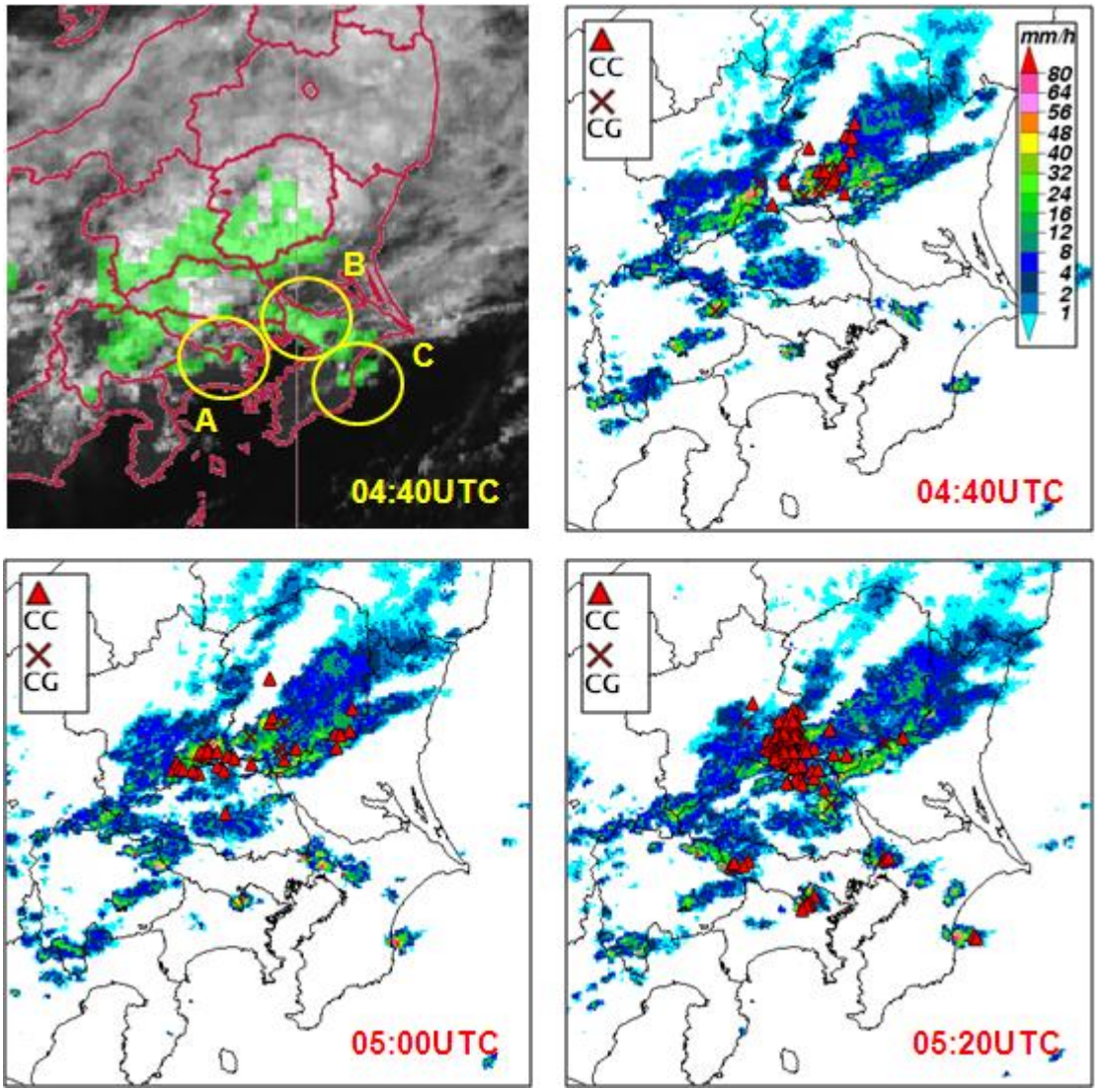

Fig3.2 lightening storm case when front goes southward. (04:40UTC Aug 26 2011)

3-1-3. Case of thunder storm observed in wide area by frontal zone. (Aug 23 2011)

Fig3.3 shows a case of Aug 23 in2011. Front stalled over Japan Sea and lightening was observed partly on the southern side of frontal zone. Strong radar echo was already observed at A, B and D and this product could detect trend of development from distribution of lightening. But detection was excessive at A. Trend of development was obscure while radar echo for precipitation was observed to some extent at C. There were Error detections at E where radar echo for precipitation was not observed. These were low level cloud which had high brightness temperature. Low level cloud which doesn't show trend of development is incidentally detected wrong by running algorithm because sensitivity for low level cloud is relatively increased noted in section 2-3-2.

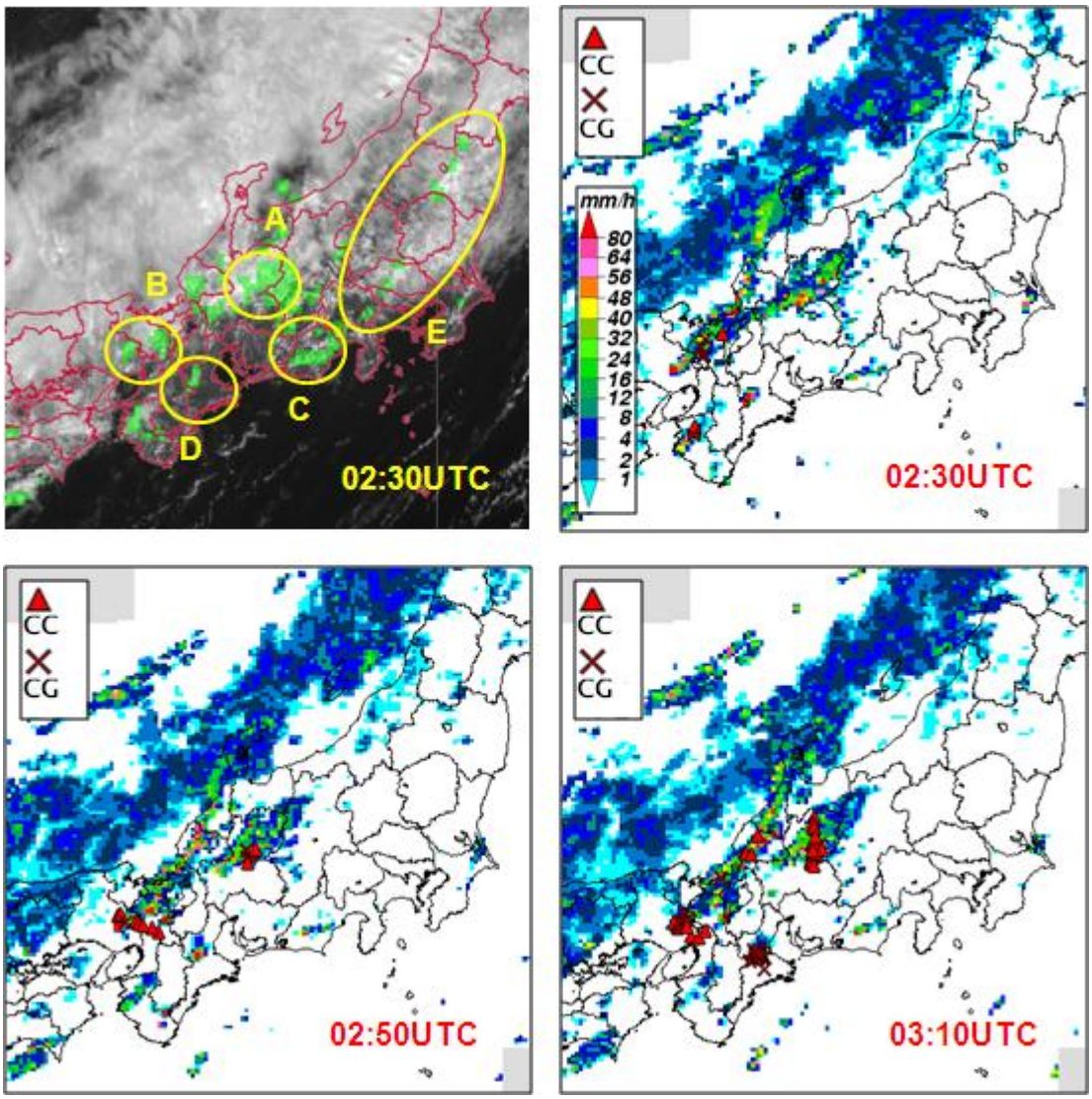

Fig3.3 Case of thunder storm observed in wide area of frontal zone.
(Aug 23 2011)

3-1-4. Case that detection is in error when upper level cloud covers low level cloud.

(July 20 in 2011)

Imager observation of geostationary satellite has limitation to presume internal cloud structure. Therefore this product adopted the specialized method for satellite imagery which is combined of time trend and surrounding information at cloud top described in chapter 2. In case that upper level cloud covers low level cloud, error detection or passed detection could occur because account for development trend of lower level cloud is difficult.

Fig3.4 shows a case around typhoon in July 20 2011. Radar echo was not observed at A and B in figure. This area was covered by upper cloud of typhoon No.6 on the sea, and the upper cloud made time variation of IR1 brightness temperature enhanced. Then detection error occurred. In the meantime strong radar echo observed even though lightening was not observed, and development trend was recognized at C in figure. However, information of lower cloud top was not gotten because of upper cloud, then detection of development trend was unable. As seen above, detection accuracy is decreased in multi layer cloud area. By the way upper air observation of Matsue station at 00UTC near A or B in figure where is rear face of typhoon indicated that CAPE is 0. In this way information related to background circumstance will fill the gap and avoidance of error detection is thought of as possible.

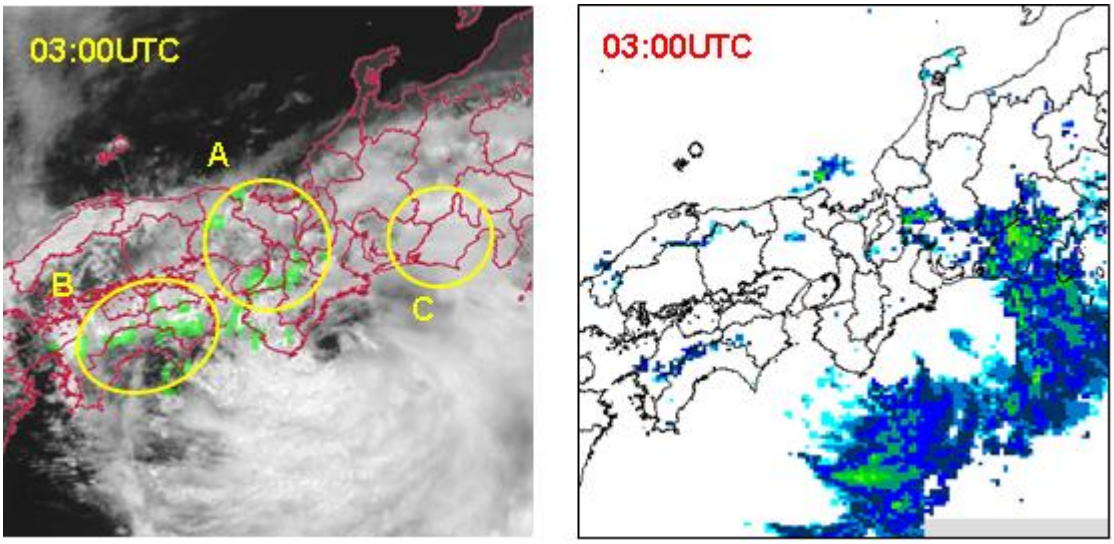

Fig3.4 Error Detection case which coexistence of lower layer cloud and upper layer cloud (03:00UTC Aug 23 2011)

3-2. Score of RDCA detection

Predictive value from June 20 to August 31 in 2011 and lead time of 86 cases for heat lightening from July to August in 2011 are calculated in order to test accuracy of RDCA. First lightening is start time of phenomenon for lead time. Lightening does not necessarily have relevance to tone of cloud development and the test is not the whole story. Predictive value is calculated in detection range of LIDEN (Fig3.5).

Concept of hit or not is described below.

I. In case that lightening is observed no later than 60 minutes within 2 grids around grid which is picked up as rapidly developing area, the detection is hit. If lightening is not observed, the detection is passed.

II. Cumulus cloud which will have lightening in future should be detected as rapidly developing area at a number of previous detection times. From this view point, if same cloud is detected as rapidly cloud area at different detection times, they are considered as independent result of detection.

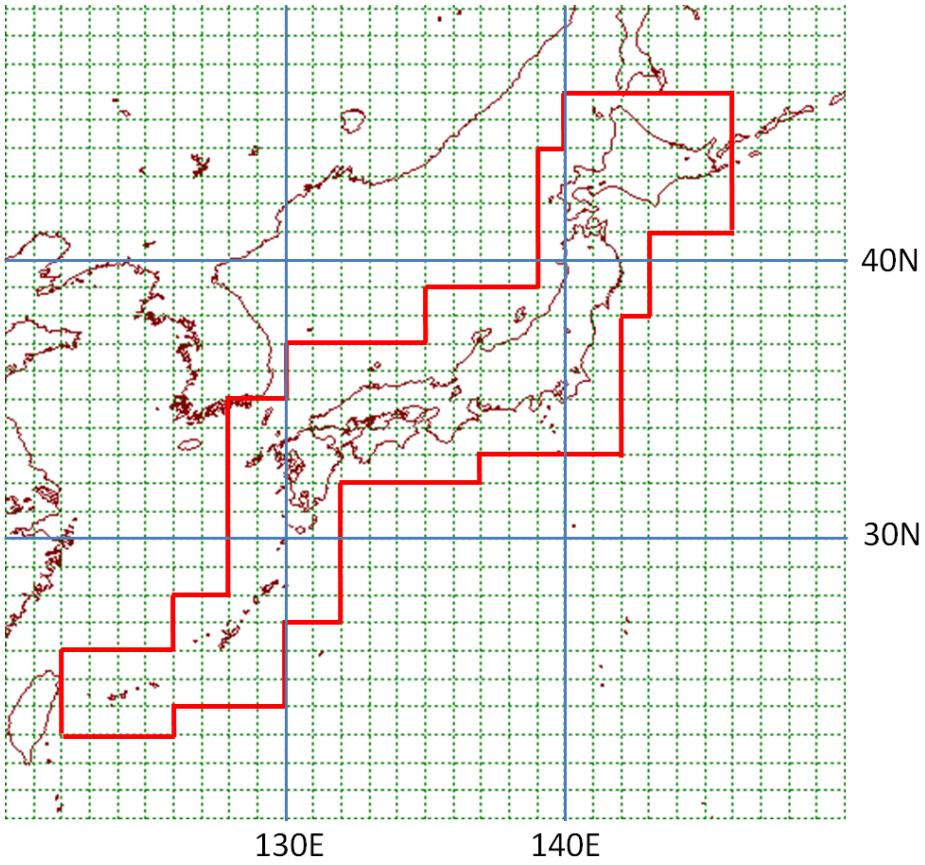

Fig3.5 Detection range of LIDEN is bounded by red line. Evaluation is performed in the area.

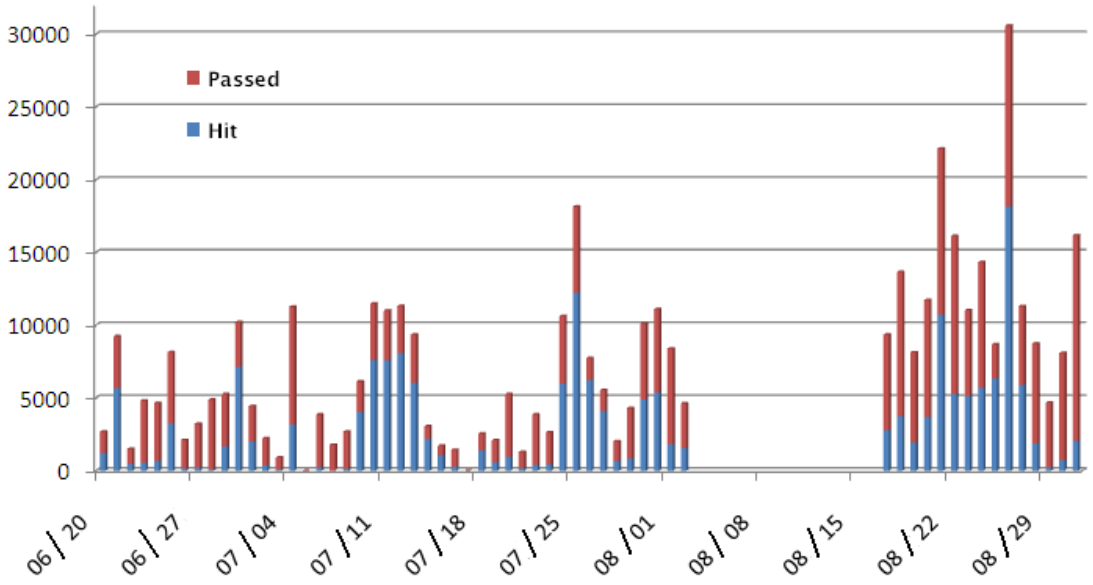

Fig3.6 Number o f hits and passed from July 20 to August 31 in 2011

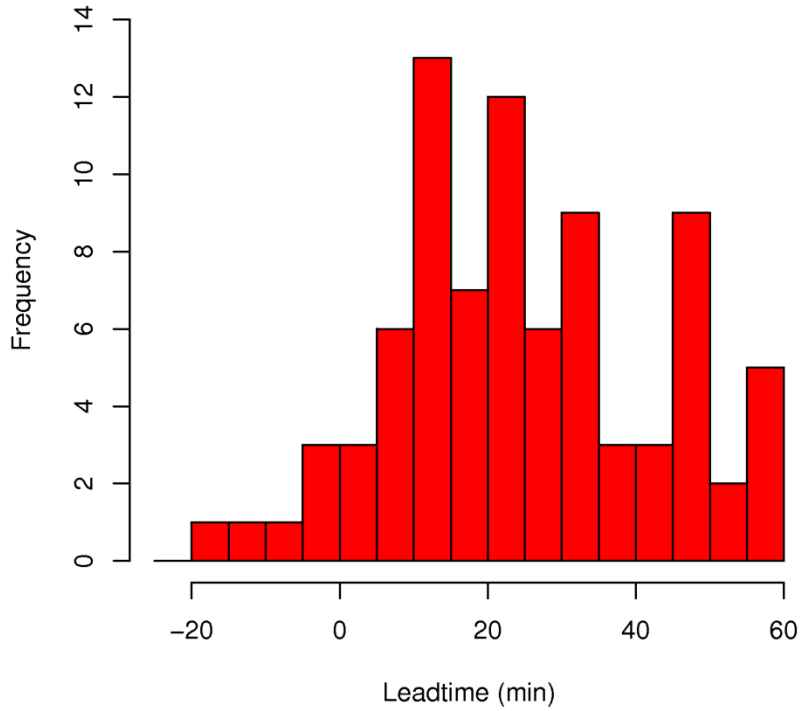

Fig. 3.7 Distribution of lead time.

86 heats lightening case is checked from July to August in 2011.

Predictive value is obtained by divided number of hits by sum of number of hits and passed. Fig3.6 shows predictive value and number of passed in each day. Rapid scan observation was cancelled from 3 to 16 in August 2011. Predictive value was 0.43 in this term. From the point of cases, predictive value is 0.68 when lightening happened often by cold trough from July 24 to 27 in 2011, predictive value is 0.45 when lightening happened often near stationary front from August 18 to 26 in 2011 and predictive value was 0.68 when heat lightening happened often under high pressure system from July 9 to 14 in 2011 though it is not independent data which was used to calculate coefficient of regression analysis.

Fig3.7 shows distribution of lead time in all cases stated before. More than 90% cases were detected as rapidly developing area before lightening and average lead time was about 20 minutes. Actually it takes a few minutes to process products and deliver its outputs, lead time users have is a few minutes shorter than 20 minutes.

3-3. Future of RDCA detection

Current algorithm is optimized for isolated heat lightening case occurred under high pressure system in summer 2011. Therefore score in situation corresponds to analogous synoptic scale is good, this product is thought to be one of helpful information. However there are also some cases which is overmuch detection. Its reasons are below.

I. This product uses only parameters obtained from satellite imagery and does not use information of synoptic scale analysis or observation data.

II. There are errors brought by calculating parameters as represented by motion cancelation.

Term I stands for that there is a space of increasing accuracy to use other observation or forecast data by contraries. The handling is available to combine other information as of now, but in future, it is thought that an integrated nowcast including method of this product and obtained index should be oriented. In term II, for example to modify method for picking up target cumulus cloud from satellite imagery and accurately tracking, further improvement is needed.

References

EUMETSAT, 2007: Update on nowcasting applications of MSG. CGMS-35 EUM-WP-27, 19 pp.

Kaufman, Y. J., and T.Nakajima, 1993: Effect of amazon smoke on cloud microphysics and albedo – analysis from satellite imagery, *J. Appl. Meteor.,* **32,** 729-744.

Mecikalski, J. R., and K. M. Bedka, 2006: Forecasting convective initiation by monitoring the evolution of moving convection in daytime GOES imagery, *Mon. Wea. Rev.,* **134,** 49-78.

MSC/JMA, 2000: Analysis and Use of Meteorological Satellite Image. Meteorological Satellite Center, 161 pp.

Nakajima, T., and M. D. King, 1990: Determination of the optical thickness and effective particle radius of clouds from reflected solar radiation measurements. Part I: Theory, *J. Atmos. Sci.,* **47,** 1878-1893.

Okabe, I., T. Imai, and Y. Izumikawa, 2011: Detection of Rapidly Developing Culumus Areas through MTSAT Rapid Scan Operation Observation, *Meteorological Satellite Center technical note,* **55,** 69-92.

Oku, Y. and H. Ishizuka, 2008: Estimate of Reflectance and an Effective Radius of Cloud Particle Using MTSAT-1R Data. *Annual of Disas. Prev. Res. Inst., Kyoto Univ.*, **51B,** 409-415 (in Japanese).

Shimoji, K., 2010: The Development for MTSAT Rapid Scan High Resolution AMVs at JMA/MSC, Proceedings of the 10th International Wind Workshop.

Rosenfeld, D., and I. M. Lensky, 1998: Satellite-Based Insights into Precipitation Formation Processes in Continental and Maritime Convection Clouds, *Bull. Amer. Meteo. Soc,* **79,** 2457-2476.